

HOW MUCH DEPTH INFORMATION CAN RADAR INFER AND CONTRIBUTE

Chen-Chou Lo and Patrick Vandewalle

EAVISE, PSI, Dept. of Electrical Engineering (ESAT), KU Leuven
Jan de Nayerlaan 5, 2860 Sint-Katelijne-Waver, Belgium

ABSTRACT

Since the release of radar data in large scale autonomous driving dataset, many works have been proposed fusing radar data as an additional guidance signal into monocular depth estimation models. Although positive performances are reported, it is still hard to tell how much depth information radar can infer and contribute in depth estimation models. In this paper, we conduct two experiments to investigate the intrinsic depth capability of radar data using state-of-the-art depth estimation models. Our experiments demonstrate that the estimated depth from only sparse radar input can detect the shape of surroundings to a certain extent. Furthermore, the monocular depth estimation model supervised by preprocessed radar only during training can achieve 70% performance in δ_1 score compared to the baseline model trained with sparse lidar.

Index Terms— depth estimation, radar, nuScenes, weak supervision, autonomous vehicle vision

1. INTRODUCTION

Depth estimation plays an essential role as a basic piece of information for applications like 3D object detection and 3D reconstruction. Thanks to the development of deep neural networks in recent years, researchers have proposed many monocular and stereo depth estimation algorithms [1, 2, 3, 4, 5, 6] with significant improvement. However, for such camera-based methods, monocular depth estimation is ill-defined that many scenes could project to the same 2D image. Stereo depth estimation is sensitive to environment lighting and texture conditions. Consequently, many works [7, 8, 9] have been proposed to leverage additional depth information as a guidance to compensate the perception of camera feature and result in a more robust and accurate performance.

Since the projected depth from lidar sensors is very accurate and high-end lidar could result in a relatively high resolution projected depth, lidar has been the most commonly used depth sensor for guiding camera-based depth estimation models. Although lidar contributes a lot of highly accurate depth information for the surroundings, it is also notorious for its high cost and sensitivity to weather conditions. On the contrary, radar is known for its robustness and reliability against extreme weather and it is much cheaper than lidar

sensors. Accordingly, several researchers start to fuse radar sensor data as a further guidance into camera-based depth estimation models [10, 11, 12, 13, 14] after the release of a large autonomous driving dataset nuScenes [15].

Existing multi-modal depth estimation methods, that integrate sparse radar with camera images, are based on the same structure of models that make use of camera images and sparse lidar. However, these lidar-fusion models are dedicated to extract features from lidar data, and projected depth from lidar and radar are quite different. These proposed radar-fusion works showed that the results improved after modifying parts of the original architectures and fusing the radar feature as additional guidance. Still, it is hard to tell to what extent the radar can contribute since radar is not only sparse but also noisy and view limited.

In this work, we investigate how much depth information radar data can infer and contribute to a depth estimation model. We conduct two sets of experiments: firstly, to predict depth by using only radar as input to demonstrate the inference capability of radar data. Secondly, to train a monocular depth estimation model with radar supervision, showing the intrinsic depth information that radar contributes. Through the experiments, we show that (1) the output prediction by radar input can capture the shape of surroundings, and (2) that a monocular depth estimation model trained with radar supervision can also estimate the depth of the surroundings to a fair extent. To the best of our knowledge, that there is no previous work investigating radar in these two aspects.

2. RELATED WORK

2.1. Depth estimation using camera and lidar

Many works have proposed to use lidar as the additional guidance signal since integration of lidar to a monocular depth estimation model can significantly improve the overall performance. Ma et al. [7] firstly integrated sparse lidar using early fusion, concatenating lidar features and camera images as input, to a CNN encoder-decoder architecture. In contrast, Jaritz et al. [16] used late fusion for lidar and camera image integration and multi-task learning to improve the performance of depth estimation. Next to the feature map fusion strategy, Vangansbeke et al. [9] used two prediction branches for both RGB and lidar input and merged into a final estima-

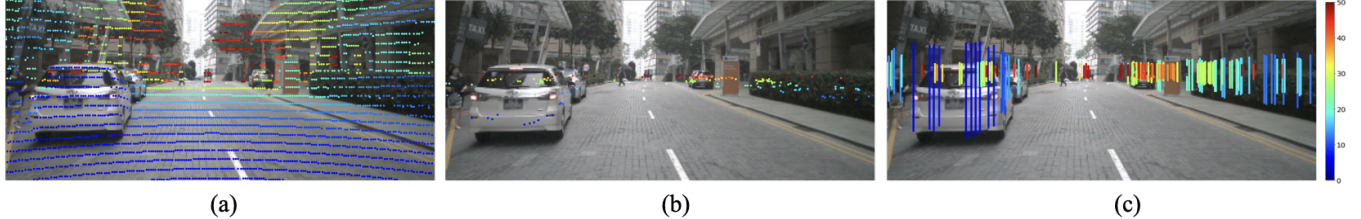


Fig. 1. Sample image from nuScenes. (a) An image with 1 sweep of sparse lidar projection; (b) 5 sweeps of raw sparse radar projection; (c) 5 sweeps of extended radar projection. All the point sizes are dilated for visualization.

tion via confidence maps. Li et al. [8] investigated supervision from multi-scale ground-truth with a cascade hourglass network to leverage the structure from different resolutions.

2.2. Depth estimation using camera and radar

On the contrary, researchers have also engaged in fusing sparse radar into depth estimation models for radar’s robustness and reliability in different conditions. Lin et al. [10] firstly conducted comprehensive experiments based on different fusion manners, and proposed a two-stage prediction method to tackle the noise in radar data. Lo and Vandewalle [11] proposed a radar preprocessing method to extend the intelligibility of radar data, and trained using late fusion and ordinal regression loss. Lee et al. [17] built upon the architecture from [10] with additional predictions for semantic segmentation and 2D object detection to improve the performance of depth estimation. Long et al. [12] proposed a radar-to-pixel association stage as a first stage, and followed by a traditional depth completion method.

All the existing depth estimation models using camera and radar data have reported promising results indicating that integrating radar can improve the accuracy of a camera-based depth estimation model. Our goal in this paper is not to introduce a new method for integrating radar and monocular depth estimation, but rather to explore the bounds of how much depth information radar data can contribute.

3. METHOD

3.1. Radar data

Although radar is a low cost and robust sensor, there are a few characteristics that bring disadvantages for radar as a depth guidance signal. As described in [10, 11, 12] in detail, the main disadvantages are sparseness, noisy measurements, and limited vertical field of view. For tackling sparseness and noise issues, Lin et al. accumulated raw radar points from multiple frames and used prediction from first-stage to do filtering on raw noisy sparse radar [10]. In this work, we directly made use of multiple-frame raw radar as one of our radar features since we have no first-stage estimation from camera images for filtering. To compensate for the limited vertical field of view, Lo and Vandewalle used the height-extended radar, extending the radar data from a point to a fixed height range

of 0.25m to 2m in world coordinates [11]. Therefore, we also used height-extended radar as another radar variation in our experiments. A visualization of these two radar formats and raw sparse lidar is shown in Fig. 1.

3.2. Architectures

To investigate how much depth information radar can infer and contribute, we conduct two types of experiments: a radar inference experiment and a radar supervision experiment. Both experiments are illustrated in Fig. 2.

3.2.1. Depth estimation with only radar input

One way to demonstrate the intrinsic depth capacity of sparse radar is to train a model that takes radar as the only input and is supervised by sparse lidar as shown in Fig. 2 (a). Thus, we make use of the depth branch from two state-of-the-art works. The depth branch module, termed $DORN_{radar}$, in [11] is a simplified modification from $DORN$ [5]. ResNet-26 [18] was used as the sparse radar feature extractor, and two 1×1 convolutional layers were concatenated after the ResNet module. After the feature map extraction, a few deconvolutional layers were used to upsample the feature map to the desired shape. The depth branch module, termed $S2D_{radar}$, in [10] used a similar architecture as the model proposed in $S2D$ [7], and the input channel of the model was changed from 4 to 1 to fit the shape of input sparse radar depth. For the decoder part, the UpProj operation was used in the upsampling layer. We make use of both models in this radar inference experiment for comparing the effectiveness of model architectures.

3.2.2. Monocular depth estimation with radar supervision

In the second experiment to show the intrinsic capacity of sparse radar to contribute depth information, we treat radar as supervised features to train a monocular depth estimation model as shown in Fig. 2 (b). In this radar supervision experiment, we use the RGB branch in [10] termed $S2D_{RGB}$. ResNet-18 was used as the RGB dense feature extractor. The whole structure is an encoder-decoder model, that uses convolutional layers to encode the input RGB feature into a latent representation and UpProj upsampling layers to decode the representation into output prediction.

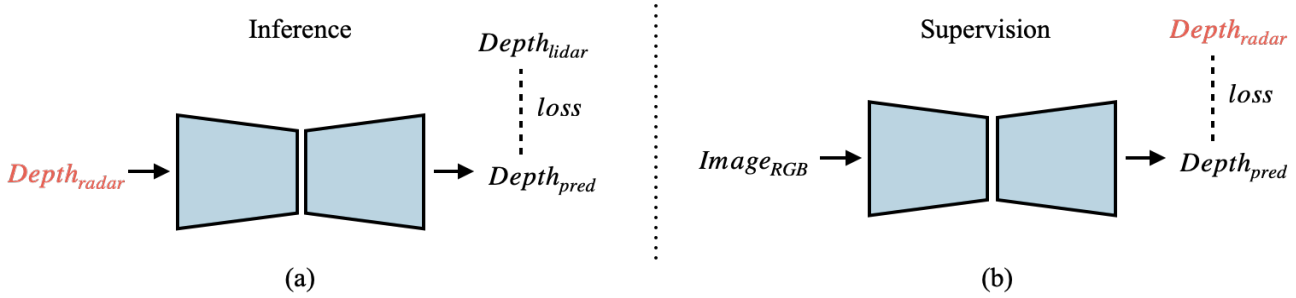


Fig. 2. Illustration of the proposed (a) radar inference experiment; (b) radar supervision experiment.

3.3. Loss functions

Since the loss functions used in the two works are different, we introduce both losses in this section. In the S2D model, the L1 loss is used as the training criteria:

$$\mathcal{L}_{L1} = \frac{1}{N} \sum_{i=0}^N |y_{pred} - y_{target}|, \quad (1)$$

where i indicates each pixel in the prediction, and y_{pred} and y_{target} are the output prediction of model and ground truth depth respectively.

On the other hand, DORN uses ordinal loss as the training criterium, which turns the regression problem into a classification problem. The ordinal loss $\mathcal{L}_{ordinal}$ is defined as the average of pixel-wise ordinal loss $\Psi(w, h, P)$ over the entire prediction:

$$\mathcal{L}_{ordinal} = -\frac{1}{N} \sum_{w=0}^{W-1} \sum_{h=0}^{H-1} \Psi(w, h, P), \quad (2)$$

$$\Psi(w, h, P) = \sum_{k=0}^{l(w, h)-1} \log(P_{(w, h)}^k) + \sum_{k=l(w, h)}^{K-1} \log(1 - P_{(w, h)}^k),$$

where (w, h) is the pixel location of the prediction of size $W \times H$. $P_{(w, h)}^k$ is the softmax probability output of location (w, h) for distance class k , and $l(w, h)$ is the target ordinal label that converted from the target depth using the spacing-increasing discretization method. Minimizing the $\mathcal{L}_{ordinal}$ will ensure the distance classification result of the prediction is close to the target label, and the model will result in a better output estimation.

Table 1. Evaluation results for radar inference experiments with different methods and input radar. (raw for 5-frame raw radar; $h - ext$ for height-extended 5-frame radar).

model	input radar	$\delta_1 \uparrow$	RMSE \downarrow	AbsRel \downarrow
DORN _{radar}	raw	0.716	7.817	0.260
	$h - ext$	0.783	6.582	0.232
S2D _{radar}	raw	0.714	8.151	0.247
	$h - ext$	0.783	6.404	0.220

Table 2. Evaluation results for radar supervision experiments. We use the RGB branch module of S2D_{RGB} in this experiment. Note that the result of sparse-lidar is the RGB baseline result from [10]

supervision signal	$\delta_1 \uparrow$	$\delta_2 \uparrow$	RMSE \downarrow	AbsRel \downarrow
sparse lidar	0.862	0.948	5.613	0.126
raw radar	0.292	0.522	18.995	0.707
height-ext radar	0.602	0.778	12.511	0.288

4. EXPERIMENTS

4.1. Dataset and implementation

nuScenes dataset. We conduct our experiments based on the nuScenes dataset [15], the most commonly used dataset for integrating radar in both depth estimation and 3D object detection tasks. The nuScenes dataset is currently one of the largest multi-modal autonomous driving dataset consisting of 6 cameras, 5 FMCW radar and a 32-beam Velodyne lidar. There are 1000 driving scenes captured in Boston and Singapore, and each scene contains roughly 40 manually synchronized samples from a 20s recording of driving. There are 850 scenes officially split into 700 and 150 as training and validation scenes respectively. We use the front view data only, and this results in 28130 training, and 6019 validation samples.

Implementation details. All the models are implemented in PyTorch and trained on a Tesla V100 GPU. To ease computation, the RGB images, projected lidar depth and radar depth are downsampled from the original shape of 900×1600 . For radar inference experiments, we downsample the input image to 450×800 and further crop into the size of 350×800 for both input and output since the upper region contributes no useful depth information. For radar supervision experiments, we use input size of 350×800 and output size of 88×200 because a model is easier to learn the overall shape on a smaller resolution of output prediction. The ground truth lidar depth for training radar inference experiments is densely interpolated with sparse lidar and RGB images by the colorization method [19] as in [11]. For both experiments, two variations of radar are used (raw and height-extended), and we accu-

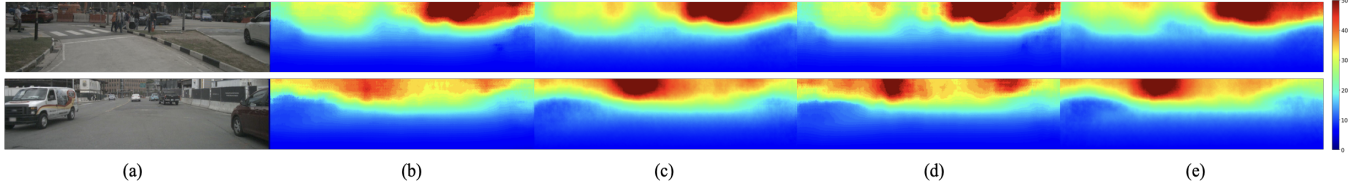


Fig. 3. Qualitative comparison of results for radar inference experiments. (a) reference RGB; output prediction from (b) $DORN_{radar}$ with raw radar input; (c) $S2D_{radar}$ with raw radar input; (d) $DORN_{radar}$ with height extended radar input; (e) $S2D_{radar}$ with height extended radar input.

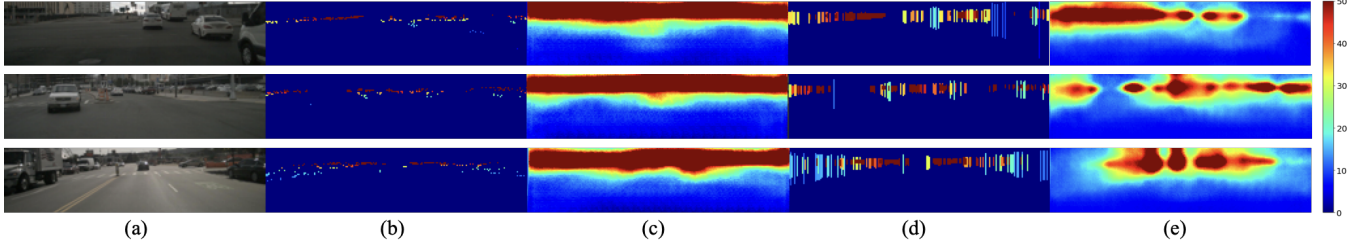


Fig. 4. Qualitative comparison of results for radar supervision experiments demonstrating improvement from training using height extended radar over raw radar. (a) input RGB; (b) raw radar; (c) prediction from model trained with raw radar supervision; (d) height extended radar; (e) prediction from model trained with height extended radar supervision.

mulate both radar data with the current frame and previous 4 frames. The height-extended radar extends each projected radar point to a height range of 0.25m to 2m. The $DORN_{radar}$ and $S2D_{radar}$ are referred from [11], [10] respectively. Polynomial decay with an initial learning rate of 0.0001 and a power rate of 0.9 is applied as the learning strategy. Batch size is set to 8, and momentum and weight decay are set to 0.9 and 0.0005 respectively. The $S2D_{radar}$ and $S2D_{RGB}$ are trained with L1 loss while $DORN_{radar}$ uses ordinal loss. All the experiments are set to train for 30 epochs on the official training splits and test on the official validation splits. The evaluation metrics used are following previous works and calculation for both experiments are based on the size of 350×800 using ground truth sparse lidar within the distance of 80m.

4.2. Radar inference experiments

This experiment takes only sparse radar as input and output a prediction with sparse lidar supervision during training. In Table 1, the evaluation results of height extended radar outperform the raw radar in all metrics on both methods. This indicates increasing the intelligibility can improve the performance. However, the result of the same radar on different methods are comparable. The qualitative result of this experiment shows in Fig. 3. It is clear that the predictions based on both radar input can detect the shape of surroundings and vehicles to a fair extent.

4.3. Radar supervision experiments

In this experiment, the model is trained with sparse radar supervision, and the output prediction is based on a RGB input.

Note that lidar was not used in this experiment. We conduct this experiment with the $S2D_{RGB}$ model. The evaluation results shown in Table 2 indicate that with properly preprocessing through height extension of radar point the overall performance improved significantly. Additionally, our result can achieve 70% of the performance in δ_1 , and RMSE and AbsRel to a fair extent compared to the result of the baseline model trained with sparse lidar supervision. The qualitative result shown in Fig. 4 also agree that the performance of the model trained with preprocessed radar improve significantly. Most of the cars and obstacles in the middle or at the edge are properly detected in Fig. 4 (e) compared to Fig. 4 (c), although it is only in a blurred shape.

5. CONCLUSION

In this paper, we conducted radar inference and supervision experiments to show how much depth information radar can infer and contribute. Our quantitative results from the inference experiment show that the inference capability of radar data is still limited after preprocessing. However, it shows an opposite trend in the radar supervision experiment. The supervision experiment revealed that a monocular depth estimation model can predict to a fair extent under the supervision of preprocessed radar. This result indicates that radar can contribute more depth information as a supervision signal after proper preprocessing, which gives a potential opportunity in weakly supervised depth estimation. To the best of our knowledge, this is the first paper to conduct such experiments to investigate the depth information of radar data.

Acknowledgements: This work was funded by a KU Leuven-Taiwan MOE Scholarship and Internal Funds KU Leuven.

6. REFERENCES

- [1] Jia-Ren Chang and Yong-Sheng Chen, “Pyramid stereo matching network,” 2018.
- [2] Feihu Zhang, Victor Prisacariu, Ruigang Yang, and Philip H.S. Torr, “Ga-net: Guided aggregation net for end-to-end stereo matching,” in *Proceedings of the IEEE/CVF Conference on Computer Vision and Pattern Recognition (CVPR)*, June 2019.
- [3] David Eigen, Christian Puhrsch, and Rob Fergus, “Depth map prediction from a single image using a multi-scale deep network,” in *Advances in Neural Information Processing Systems*, Z. Ghahramani, M. Welling, C. Cortes, N. Lawrence, and K. Q. Weinberger, Eds. 2014, vol. 27, pp. 2366–2374, Curran Associates, Inc.
- [4] D. Eigen and R. Fergus, “Predicting depth, surface normals and semantic labels with a common multi-scale convolutional architecture,” *2015 IEEE International Conference on Computer Vision (ICCV)*, pp. 2650–2658, 2015.
- [5] Huan Fu, M. Gong, C. Wang, K. Batmanghelich, and D. Tao, “Deep ordinal regression network for monocular depth estimation,” *2018 IEEE/CVF Conference on Computer Vision and Pattern Recognition*, pp. 2002–2011, 2018.
- [6] Jin Han Lee, Myung-Kyu Han, Dong Wook Ko, and Il Hong Suh, “From big to small: Multi-scale local planar guidance for monocular depth estimation,” *arXiv preprint arXiv:1907.10326*, 2019.
- [7] Fangchang Ma and S. Karaman, “Sparse-to-dense: Depth prediction from sparse depth samples and a single image,” *2018 IEEE International Conference on Robotics and Automation (ICRA)*, pp. 1–8, 2018.
- [8] Ang Li, Zejian Yuan, Yonggen Ling, Wanchao Chi, shenghao zhang, and Chong Zhang, “A multi-scale guided cascade hourglass network for depth completion,” in *Proceedings of the IEEE/CVF Winter Conference on Applications of Computer Vision (WACV)*, March 2020.
- [9] Wouter Van Gansbeke, Davy Neven, Bert De Brabandere, and Luc Van Gool, “Sparse and noisy lidar completion with rgb guidance and uncertainty,” in *2019 16th International Conference on Machine Vision Applications (MVA)*, 2019, pp. 1–6.
- [10] Juan-Ting Lin, Dengxin Dai, and Luc Van Gool, “Depth Estimation from Monocular Images and Sparse Radar Data,” in *IEEE International Conference on Intelligent Robots and Systems (IROS)*, 2020.
- [11] Chen-Chou Lo and Patrick Vandewalle, “Depth estimation from monocular images and sparse radar using deep ordinal regression network,” in *2021 IEEE International Conference on Image Processing (ICIP)*, 2021, pp. 3343–3347.
- [12] Yunfei Long, Daniel Morris, Xiaoming Liu, Marcos Castro, Punarjay Chakravarty, and Praveen Narayanan, “Radar-camera pixel depth association for depth completion,” in *Proceedings of the IEEE/CVF Conference on Computer Vision and Pattern Recognition (CVPR)*, June 2021, pp. 12507–12516.
- [13] Wei-Yu Lee, Ljubomir Jovanov, and Wilfried Philips, “Semantic-guided radar-vision fusion for depth estimation and object detection,” in *32th British Machine Vision Conference (BMVC)*, November 2021, pp. 1–13.
- [14] Muhamamd Ishfaq Hussain, Muhammad Aasim Rafique, and Moongu Jeon, “Rvmde: Radar validated monocular depth estimation for robotics,” 2021.
- [15] H. Caesar, Varun Bankiti, A. Lang, Sourabh Vora, Venice Erin Lioung, Q. Xu, A. Krishnan, Yu Pan, Giancarlo Baldan, and Oscar Beijbom, “nuscenes: A multimodal dataset for autonomous driving,” *2020 IEEE/CVF Conference on Computer Vision and Pattern Recognition (CVPR)*, pp. 11618–11628, 2020.
- [16] M. Jaritz, Raoul de Charette, É. Wirbel, Xavier Perrotton, and F. Nashashibi, “Sparse and dense data with cnns: Depth completion and semantic segmentation,” *2018 International Conference on 3D Vision (3DV)*, pp. 52–60, 2018.
- [17] Wei-Yu Lee, Ljubomir Jovanov, and Wilfried Philips, “Semantic-guided radar-vision fusion for depth estimation and object detection,” 2021.
- [18] Kaiming He, X. Zhang, Shaoqing Ren, and Jian Sun, “Deep residual learning for image recognition,” *2016 IEEE Conference on Computer Vision and Pattern Recognition (CVPR)*, pp. 770–778, 2016.
- [19] Anat Levin, Dani Lischinski, and Yair Weiss, “Colorization using optimization.,” *ACM Trans. Graph.*, vol. 23, no. 3, pp. 689–694, 2004.